Cancer Letters 362 (2015) 218–228

Contents lists available at ScienceDirect

Cancer Letters

journal homepage: www.elsevier.com/locate/canlet

Original Articles

# Molecular characterization of 7 new established cell lines from high grade serous ovarian cancer

Caroline Kreuzinger [a], Magdalena Gamperl [a], Andrea Wolf [a], Georg Heinze [b], Angelika Geroldinger [b], Diether Lambrechts [c,d], Bram Boeckx [c,d], Dominiek Smeets [c,d], Reinhard Horvat [e], Stefanie Aust [a], Gerhard Hamilton [f], Robert Zeillinger [a,f], Dan Cacsire Castillo-Tong [a,*]

[a] Molecular Oncology Group, Department of Obstetrics and Gynecology, Comprehensive Cancer Center, Medical University of Vienna, Waehringer Guertel 18-20, 5Q, A-1090 Vienna, Austria
[b] Center for Medical Statistics, Informatics and Intelligent Systems, Medical University of Vienna, Vienna, Austria
[c] Vesalius Research Center, VIB, Leuven, Belgium
[d] Laboratory for Translational Genetics, Department of Oncology, KU Leuven, Leuven, Belgium
[e] Department of Clinical Pathology, Medical University of Vienna, Vienna, Austria
[f] Ludwig Boltzmann Cluster of Translational Oncology, Vienna, Austria

ARTICLE INFO

*Article history:*
Received 12 November 2014
Received in revised form 23 March 2015
Accepted 31 March 2015

*Keywords:*
Cell line
High grade serous ovarian cancer
Platinum
*TP53*
*BRCA*

ABSTRACT

Cancer cell lines are good *in vitro* models to study molecular mechanisms underlying chemoresistance and cancer recurrence. Recent works have demonstrated that most of the available ovarian cancer cell lines are most unlikely high grade serous (HGSOC), the major type of epithelial ovarian cancer. We aimed at establishing well characterized HGSOC cell lines, which can be used as optimal models for ovarian cancer research.

We successfully established seven cell lines from HGSOC and provided the major genomic alterations and the transcriptomic landscapes of them. They exhibited different gene expression patterns in the key pathways involved in cancer resistance. Each cell line harbored a unique *TP53* mutation as their corresponding tumors and expressed cytokeratins 8/18/19 and EpCAM. Two matched lines were established from the same patient, one at diagnosis and being sensitive to carboplatin and the other during chemotherapy and being resistant. Two cell lines presented respective *BRCA1* and *BRCA2* mutations.

To conclude, we have established seven cell lines and well characterized them at genomic and transcriptomic levels. They are optimal models to investigate the molecular mechanisms underlying the progression, chemo resistance and recurrence of HGSOC.



## Introduction

Epithelial ovarian cancer (EOC) is the most lethal type of ovarian cancer and accounts for 4% of cancer deaths in women [1]. High grade serous ovarian cancer (HGSOC) is the most frequent histological type, accounting for about 70% of all EOC [2]. Standard therapies include surgery and platinum-based chemotherapy. Although most of the patients show complete clinical response after the first-line treatment, nearly all of them relapse and develop resistant disease which eventually causes death. The very high rate of resistance and early recurrence are the major reasons for the very low 5-year survival rate of around 30% [3].

Platinum-based drugs bind to DNA, produce inter- and intrastrand adducts and ultimately induce cell death. The mechanisms of platinum resistance and recurrence of HGSOC are not completely understood [4]. Various pathways have been proposed to be involved in platinum resistance [5] including DNA repair [6–10], cell cycle control and apoptosis [11,12]. Despite the fact that p53 plays a central role in most of these processes and that almost all HGSOC harbor mutations in the *TP53* gene [13], no direct link between *TP53* mutations and carboplatin resistance could be determined so far.

It is thus of utmost importance to identify key genes or pathways involved in platinum resistance to open the way to develop new drugs to be used alone or in combination with platinum to eliminate the tumor mass along with resistant cells [14].

Cancer cell lines are good *in vitro* models to study molecular mechanisms underlying chemoresistance and tumor recurrence, provided that they have been well characterized [15]. For decades, cell lines have been used to generate our knowledge on ovarian cancer.

* Corresponding author. Tel.: +43 1 4040078330; fax: +43 1 4040078320.
*E-mail address:* dan.cacsire-castillo@meduniwien.ac.at (D. Cacsire Castillo-Tong).

http://dx.doi.org/10.1016/j.canlet.2015.03.040

However, previously established cell lines are insufficiently characterized, missing important information on tumors and genomic characteristics such as histopathological type, clinical outcome of the patients and *TP53* mutation status. A systematic genomic analysis on a panel of 47 ovarian cancer cell lines and the comparison with the TCGA dataset suggested that most of the commonly used "ovarian cancer" cell lines were most unlikely to originate from HGSOC and thus are not optimal models for studying the disease [16]. Furthermore, discrepancies and difficulties in identifying cell origin, histological type, mutation status or clinical data of the donor patients in different cell banks question the use of the available cell lines as proper models of HGSOC [15,17].

A considerable study on tumor heterogeneity and clonal evolution in ovarian cancer has been performed [18] using matched cell lines established at the end of the 1980s [19] and new cell line series derived from the same patient have been established and characterized [20,21]. These approaches provide new opportunities to study HGSOC. However, the unavailability of histopathological confirmation, the non-standard treatment and lack of information on patients' clinical outcome are still persisting obstacles. New cell lines with well-defined molecular and cellular characteristics, complete clinical documentation of the corresponding tumors and the patients are urgently needed. Particularly, matched cell lines established from tumor materials taken from different time points from the same patient will certainly provide advantages to study the clonal evolution of tumor cells.

In this work, we established cell lines from ascites or tumor tissue from patients with HGSOC, and characterized them regarding gene mutations, mRNA expression, protein expression and chemosensitivity.

## Materials and methods

### *Patients and clinical materials*

Informed consents were obtained from all patients with HGSOC included in this study in the Department of Obstetrics and Gynecology, Medical University of Vienna. The study protocol was approved by the ethics committees (EK Nr. 366/2003 and 260/2003). During cytoreductive surgery, tumor tissues were directly transferred to the Department of Pathology, Medical University of Vienna. After confirming the histological type, the materials were sent to the laboratory. Ascites was collected from the clinic and directly sent to the laboratory. The clinical response of the patients was evaluated following the standard guidelines [22].

### *Establishment and maintenance of cell lines*

Ascites was centrifuged and the red blood cells were depleted with a centrifugation step with Histopaque 1077 (Sigma-Aldrich, St. Louis, USA).

Tumor tissues were cut into small pieces and digested with collagenase (1 mg/mL, 1453 CDU/mg, Sigma-Aldrich) at 37 °C for about 1 h.

Cells were cultivated in DMEM medium, with 10% fetal bovine serum (FBS), 100 units/mL penicillin and 100 µg/mL streptomycin (PS; all from Gibco by Life Technologies, CA, USA) at 37 °C and 5% $CO_2$.

VenorGeM Classic Mycoplasma Detection Kit for conventional PCR (Minerva Biolabs, Berlin, Germany) was used to control mycoplasma contaminations.

### *Authentication of cell lines*

Short tandem repeat (STR) analyses of 7 markers (TPOX, vWA, CSF180, D16S539, D7S820, D13S317, D5S818, Applied Biosystems Life Technologies) were performed using ABI Prism 310 Genetic Analyzer (Applied Biosystems, Life Technologies).

### *Scratch assay*

Cell culture at 100% confluency was scratched with a Pasteur pipette and pictures were taken at the time of scratching and 48 h afterwards. The web based Software WimScratch (ibidi, Munich, Germany) was used to determine the confluency of the cells on the scratched area. The scratched surface in each cell culture flask was defined as 100% and the proportion of the remaining cell free area after 48 h was calculated.

### *DNA and RNA isolation*

Homogenized fresh frozen tumor tissue (Mikro-Dismembrator U; B.Braun Biotech International, Melsungen, Germany) lysate and cell pellet lysate were processed for DNA and RNA isolation using the AllPrep DNA/RNA Mini Kit (Qiagen, Hilden, Germany). The nucleic acid concentrations were measured by a BioPhotometer (Eppendorf, Hamburg, Germany).

### *Determination of gene mutation*

*TP53* mutation was determined by a modified p53 functional yeast assay [23,24], and Sanger sequencing. In addition, ddPCR systems for each unique *TP53* mutation were established to determine the percentage of the *TP53* mutant cells in cell culture (Table 1).

*BRCA1 and BRCA2* mutations were determined by Sanger sequencing [25].

Hot spot mutations in *KRAS* (c.35G>C, c.34G>C, c.35G>A, c.34G>T, c.34G>A; 35G>T, c.34G>C; 35G>T, c.34G>A, c.35G>T, c.38G>A, c.37G>T) and *BRAF* (V600E, c.1799T>A) were examined with a reverse oligonucleotide hybridization assay (KRAS-BRAF StripAssay (ViennaLab Diagnostics GmbH, Vienna, Austria)).

### *Immunohistochemical staining (IHC)*

Formalin fixed paraffin embedded (FFPE) tissues were sectioned at 3 µm. The IHC was performed with the Dako LSAB+ System-HRP kit (Code K0690; Dako, CA, USA) and all steps were performed according to the manufacturer's instructions.

Cytospin preparations were fixed in 4% formaldehyde and incubated with 0.5% X Triton X-100 for 10 min before further processed.

Primary antibodies were diluted with Dako REAL Antibody diluent (Agilent Technologies, St. Clara, California) and incubated overnight at 4 °C. FLEX Negative Control Mouse Cocktail (Agilent Technologies) and Negative Control Rabbit IgG (Biocare Medical, Concord, USA) were used as isotype controls.

Nuclei were stained with hematoxylin solution modified according to Gill III (Merck Millipore Darmstadt, Germany) before mounting the slide with Kaisers Glyceringelatine (Merck Millipore).

Antibodies: anti-cytokeratin 8/18/19 (IgG1, mouse, clone A45-B/B3; AS Diagnostik, Hueckeswagen, Germany) at 1:100; anti-vimentin, ready to use (CONFIRM Anti-vimentin (V9) Primary Antib, Ventana, Roche Diagnostics, Basel, Switzerland); CD44 (IgG1, mouse, clone 8E2F3; ProMab, Richmond, USA) at 1:4000; EpCAM (IgG, rabbit, clone E144; abcam, Cambridge, UK) at 1:300; CA125 (IgG, rabbit, clone OV185:1; Leica Biosystems, Nussloch, Germany) at 1:200.

The staining was scored by a semi quantitative method as described previously [26].

### *In vitro chemosensitivity assay*

A total of $1 \times 10^4$ cells/well were seeded in 96-well plates. Carboplatin (Enzo Life Sciences, NY, USA) at concentrations of 20, 10, 5, 2.5, 1.25, 0.6, 0.3, 0.16, 0.08, and 0.04 µg/mL was added in quadruplicates. Cells were incubated at 37 °C and 5% $CO_2$

**Table 1**
ddPCR systems for individual *TP53* mutation.

| Mutation | Forward primer | Reverse primer | Probe 1 FAM | Probe 2 VIC |
|---|---|---|---|---|
| Cd_del170 | 5′-cgccatggccatctacaag-3′ | 5′-gctcaccatcgctatctgagc-3′ | 5′-FAM-agcacatggaggttg-3′-MGB | 5′-VIC-gcacatgacggaggt-3′-MGB |
| Cd_187_Intron Splice site, ggt>gat | 5′-gcagtcacagcacatgacgg-3′ | 5′-cagtgaggaatcagaggcctg-3′ | 5′-FAM-agatagcgatgatgagc-3′-MGB | 5′-VIC-agatagcgatggtgagc-3′-MGB |
| Cd_193, cat>cct | 5′-ccaggcctctgattcctcac-3′ | 5′-catagggcaccaccacactatg-3′ | 5′-FAM-tcctcagcctcttat-3′-MGB | 5′-VIC-tcctcagcatctta-3′-MGB |
| Cd_273, cgt>cat | 5′-gtggtaatctactgggacgg-3′ | 5′-cggagattctcttcctctgt-3′ | 5′-FAM-tgaggtgcatgtttg-3′-MGB | 5′-VIC-tgaggtgcgtgtttg-3′-MGB |
| Cd_333-del c | 5′-gtcagctgtataggtacttgaagtgcag-3′ | 5′-gctctcggaacatctcgaagc-3′ | 5′-FAM-ctgcagatcgtgggc-3′-MGB | 5′-VIC-gcagatccgtgggc-3′-MGB |
| Cd_340_343, gag-del10-ag-ctg | 5′-ctcctctgttgctgcagatcc-3′ | 5′-ctggagtgagccctgctcc-3′ | 5′-FAM-cttcgagagctgaatg-3′-MGB | 5′-VIC-cttcgagatgttccgagag-3′-MGB |

for 96 h. Cell viability was measured by a MTT assay (EZ4U, Salem, NH, USA). $IC_{50}$ values were calculated using Origin Software V8.1 (OriginLab, Northampton, MA, USA).

*Low coverage whole genome sequencing*

Shot-gun whole genome libraries were prepared using KAPA library preparation kit (KAPA Biosystems) according to the manufacturer's instructions, quantified for the PCR products, and sequenced on a HiSeq2000 (Illumina) at low coverage generating 50 bp reads. Raw sequencing reads were mapped to the human reference genome (NCBI37/hg19) using Burrows–Wheeler Aligner (BWA v0.5.8a). On average, 12 719 610 reads were mapped. PCR duplicates were removed by Picard (v1.43) resulting in an average of 12 340 052 reads (3% duplicates). Using the QDNAseq package v. 1.0.5 [27], copy-number alterations were identified by binning the reads in 100 kb windows. Bins in problematic regions were blacklisted. Read counts were corrected for GC-content and mappability using LOESS regression and then normalized by the median with the outliers smoothed. Segmentation of the bin values was performed by ASCAT v. 2.0.7 [28].

*RNA-sequencing, analysis and annotation*

RNA libraries were created using the Illumina TruSeq RNA sample preparation kit V2 according to the manufacturer's instructions and sequenced on a HiSeq2000 (Illumina) using a V3 flowcell generating $1 \times 50$ bp reads. Raw sequencing reads were mapped to the transcriptome and the human reference genome (NCBI37/hg19) using TopHat 2.0 [29] and Bowtie 2.0 [30]. On average 32 859 670 reads were assigned to genes with the HTSeq software package and normalized with EDASeq [31,32].

To present the transcriptomic landscape of the cell lines, we selected relevant genes from important pathways in three pathway databases (KEGG, BioCarta, PANTHER). Logarithmized read counts are visualized in a heatmap produced with R (http://www.r-project.org) using the package heatmap.plus. Within each pathway, genes are sorted by geometric mean read count. Clustering of cell lines was expressed by a dendrogram using the Euclidean distance and the default clustering algorithm.

## Results

*Patients and tumor characteristics*

Seven cell lines from six patients with HGSOC were established. One cell line 8587 was derived from tumor tissue and all others were from ascites. Two cell lines, 13363 and 15233, were derived from the same patient with the first one taken at diagnosis and the second one under the treatment. The age of the patients at diagnosis ranged from 33 to 67 with a median age of 55. All primary samples set for cell culture were taken before any chemotherapy.

All patients received standard treatments and presented different clinical response to the first line chemotherapy (Table 2, Fig. 1).

*Cell lines*

In ascites, tumor cells often appeared in form of clusters, which were easily separated and purified by filtration. In some primary cultures, tumor cells formed an island-like structure surrounded by fibroblasts (Fig. 2I) which mimicked the tumor structure *in vivo*. The fibroblasts were reduced and finally eliminated by repeating selective trypsinization, until pure tumor cell culture was obtained (Fig. 2H). All cell lines have been passaged more than 35 times.

After *TP53* mutations were determined by the functional yeast assay in the corresponding tumor tissues, the purity of the cell culture was determined using ddPCR. A cell line was defined when the culture reached a 100% purity of specific *TP53* mutant cells. STR

**Table 2**
Data of patients and characteristics of tumors.

| Clinical parameters | Patient | | | | | | |
|---|---|---|---|---|---|---|---|
| | 12370 | 13363 | 15233 | 13699 | 13914_1 | 14433_1 | 8587 |
| Age at diagnosis | 67 | 33 | | 53 | 66 | 61 | 49 |
| Histological type | Serous | Serous | | Serous | Serous | Serous | Serous |
| Grade | 3 | 3 | | 3 | 3 | 3 | 3 |
| FIGO | IIIC | IV | | IIIC | IIIC | IV | IIIB |
| Rest tumor | >5 cm | <5 mm | | 0 | 0 | 0 | 0 |
| Neoadjuvant therapy | Carboplatin/Paclitaxel | Carboplatin/Paclitaxel | | No | No | Carboplatin/Paclitaxel | No |
| Cycles | 3 | 3 | | | | 6 | |
| 1st adjuvant therapy | Carboplatin/Paclitaxel+ Cisplatin/Gemcitabine | Carboplatin/Paclitaxel | | Carboplatin/ Paclitaxel | Carboplatin/ Paclitaxel | Carboplatin/Paclitaxel | Carboplatin/ Paclitaxel |
| Cycles | 6 + 1 | 8 | | 6 | 6 | 2 | 6 |
| Response at the completion of therapy | cPR | cPR | | cCR | cCR | cCR | cCR |
| Response 6 months after treatment | Not applicable | cPD | | cCR | cCR | cPD | cCR |
| Previous history of cancer | None | None | | None | Breast cancer (IDC, g1) at ages 48 and 65 | None | None |
| Follow up (date of last platinum dose from 1st line to last medical contact) | Died 3 months after | cPR during 2nd chemotherapy, died 9 months after | | 16 months | 15 months | 7 months | 17 months |
| *TP53* mutation | g.13339 t > g (His193Pro) | g.13187_13189 del cgt (Thr170) | | g.17575 del c, (Arg333Val fsX12) | g.17596_17605 del (Met340Ser fsX2) | g.13239 g > a (Gly187Asp)[a] | g.14487 g > a (Arg273His) |
| Mutation type | Missense | Deletion | | Frameshift causing a truncated protein | Frameshift causing a truncated protein | Frameshift causing a truncated protein | Missense |
| Localization of mutation | DBD | DBD | | OD | OD | DBD | DBD |
| *BRCA1/2* mutation | None | None | | None | BRCA1 c.3481_3491 del (Glu1161 fsPheX3) | BRCA2 c.8557a>t (Lys2853X) | None |
| Mutation type | | | | | Frameshift causing a truncated protein | Nonsense mutation causing a truncated protein | |

[a] Point mutation at intron 5 (bp 13239) leading to a variant splicing (g.13193_13238del, Val172Val), which causes a frameshift and a truncated protein (fsX60).
cPR: clinical partial response; cCR: clinical complete response; cPD: clinical progressive disease; DBD: central DNA-binding core domain; OD: homooligomerization domain.

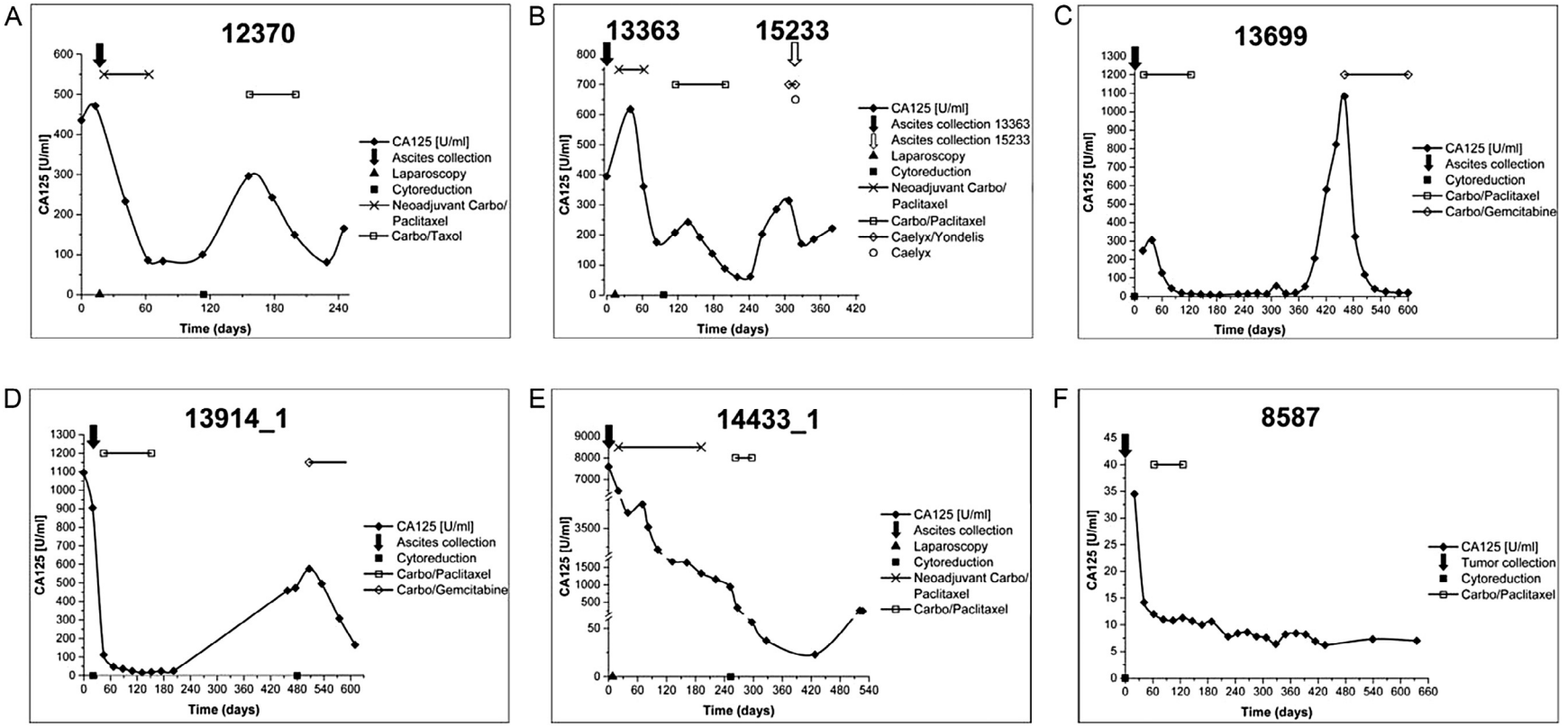


**Fig. 1.** CA125 plasma course of the patients. Time of collecting ascites or tumor tissues, operation, and chemotherapeutical treatment were indicated. A: 12370; B: 13363 and 15233; C: 13699; D: 13914_1; E: 14433_1; F: 8587.

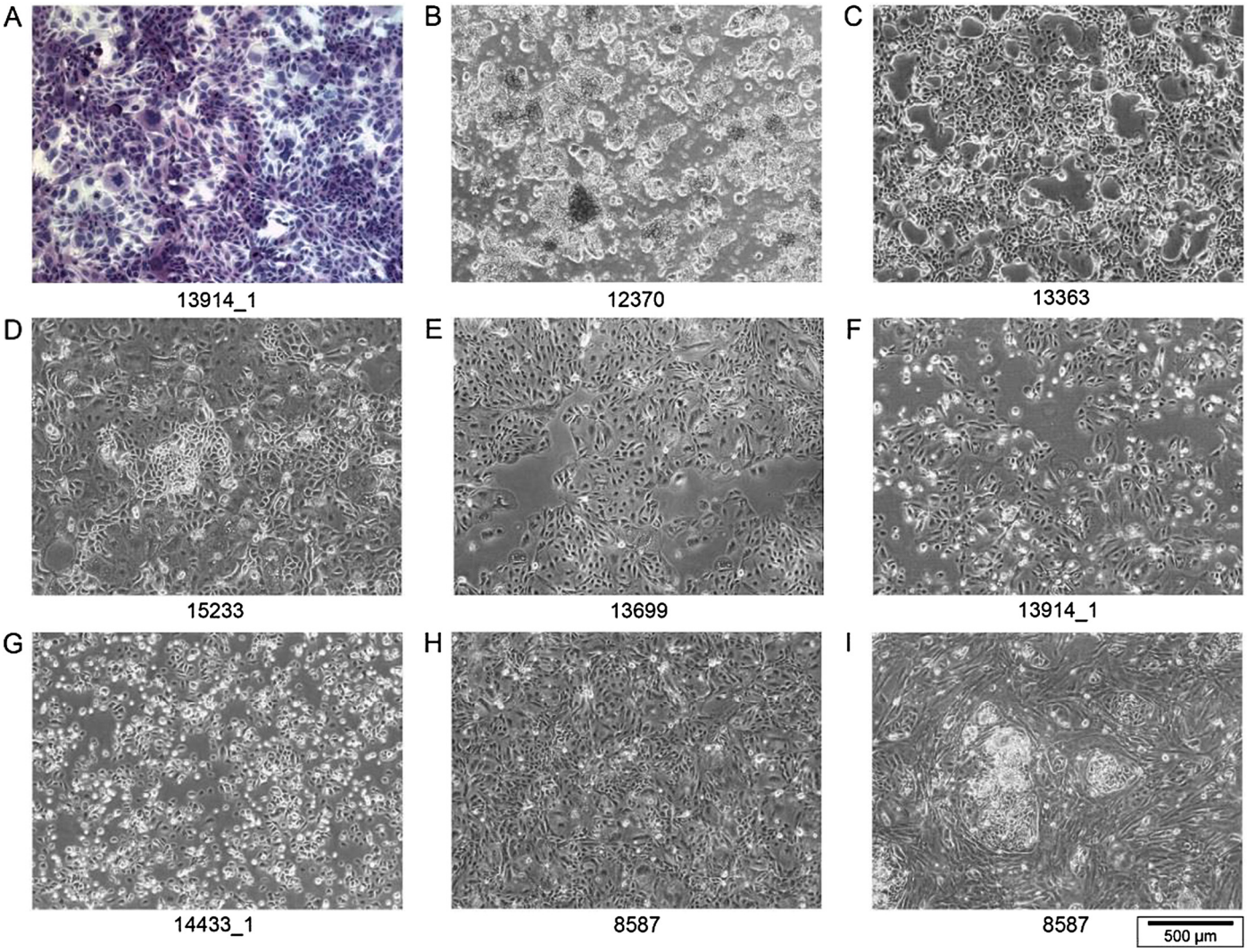


**Fig. 2.** Morphology of cells (brightfield microscopy). A: HE staining of 13914_1; B: 12370; C: 13363; D: 15233; E: 13699; F: 13914_1; G: 14433_1; H: 8587 in pure culture; I: 8587, showing tumor cell islands surrounded by fibroblasts.

analyses were performed regularly to confirm the cell authenticity and to avoid the cross contamination of cell lines, which is a frequent problem in cell culture [33].

*Morphology*

All cell lines had a polymorphic appearance (Fig. 2). They presented with irregular sizes and shapes and had a high nucleus to cytoplasm ratio (Fig. 2A).

Six cell lines grew in monolayer. One cell line (12370) grew as a mixture of clusters and adherent "islands". These clusters could contain a couple of cells up to several hundred cells (Fig. 2B).

*Growth and mobility*

Split ratios of the cell lines differed from 1:2 to 1:3. Some cell lines had a doubling time of 2–3 days (13363, 13699, 14433_1) whereas others doubled in 6–9 days (12370, 15233, 13914_1, 8587).

Scratch assays showed that one cell line (13699) did not have any mobility (Fig. 3D) while other lines had a similar migration rate, filling around 1/3–4/5 of the scratched areas within 48 h (Fig. 3A–C,E–G). The two cell lines derived from the same patient (13363 and 15233) had similar high migration ability (Fig. 3B,C).

*Genomic characteristics*

Somatic *TP53* mutations were found in tumors from all patients. Sites of mutations and their consequence are presented in Table 2. Sanger sequencing of the corresponding blood DNA confirmed that none of the patients had a germline *TP53* mutation. All cell lines were proved to have the same mutation as their corresponding tumors homozygously. ddPCR confirmed that the *TP53* mutations were stable throughout all passages.

Additionally, homogeneous mutations in the *BRCA2* and *BRCA1* genes were found in the cell lines 14433_1 and 13914_1, respectively. Sanger sequencing of the corresponding germline DNA showed that these mutations were already present as heterozygous mutations (Table 2).

No mutations in the *KRAS* and *BRAF* genes were detected in the cell lines.

Analysis of the copy number alterations with low-coverage whole genome sequencing revealed a high degree of chromosomal instability in each cell line (Fig. 4), which was expected for HGSOC. Noticeably, focal amplifications affecting *PIK3CA* were observed in 6/7 cell lines, but not in the 12370. *BRAF* and *MYC* were also found amplified albeit not frequently. *TP53*, *BRCA1* and BRCA2 were frequently affected by deletions. The presence of homozygous mutation

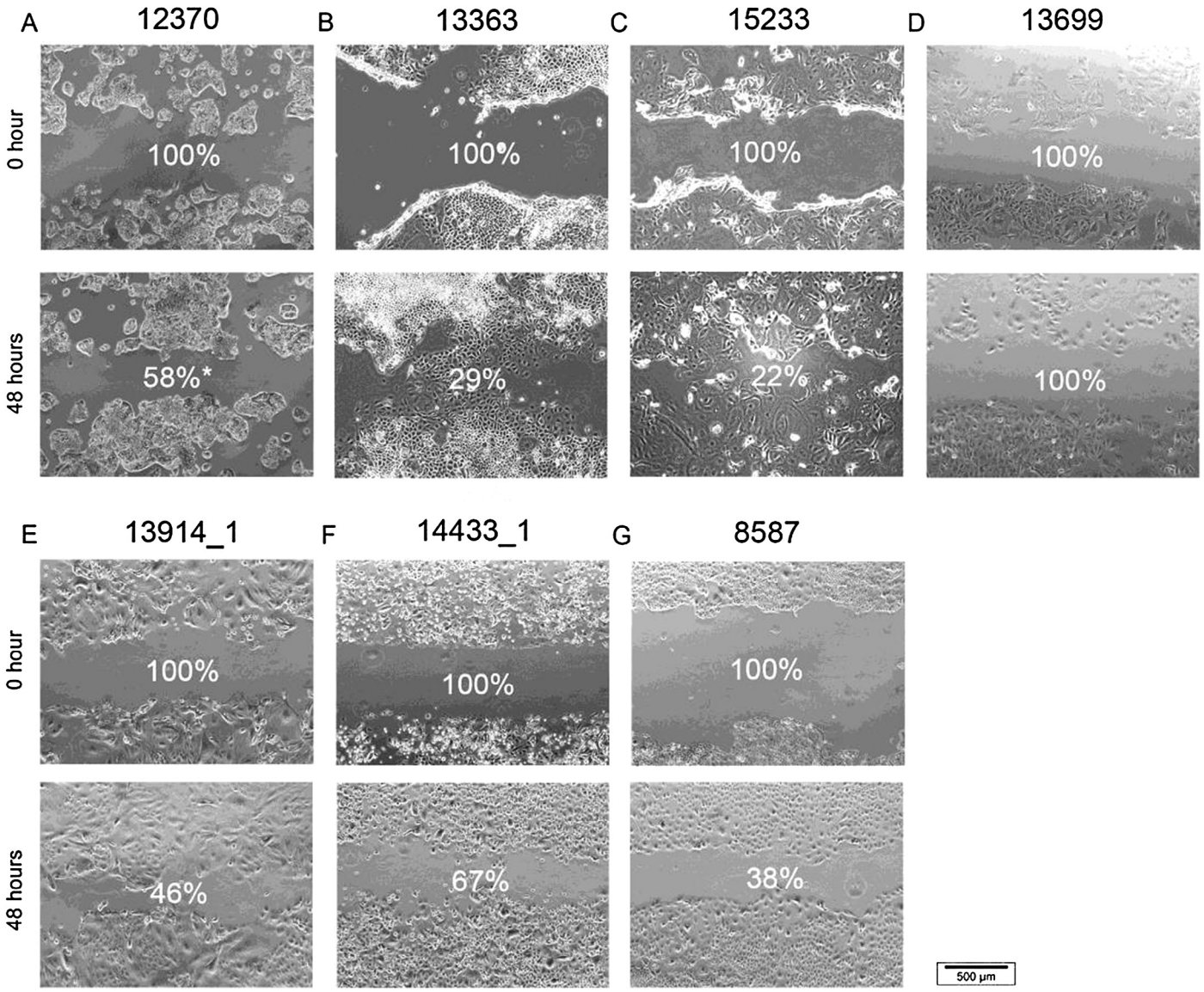


**Fig. 3.** Scratch assays showing cell mobility. Pictures were taken at 0 h and 48 h after scratching (brightfield microscopy). The scratched area at 0 h was defined as 100%; the percentage of the remaining cell free area was indicated at 48 h. A: 58%* remaining cell free area was manually calculated because of cell clustering.

in *TP53* indicated loss of heterogeneity (LOH) on chromosome 17 in tumor cells, which aligned with LOH of the *BRCA1*. The mutations in *BRCA1* and *BRCA2* were heterozygous in germ-line but homozygous in the cell line, again indicating the LOH in this region (Fig. 4F,G).

*Landscape of gene expression*

Gene expression profiles of key pathways are shown in Fig. 5. The cell lines presented dominant epithelial cell phenotype, with elevated expression of the epithelial markers like *KRT8/18/19* and *EpCAM*, and low expression of the principal mesenchymal markers. They also showed uniformly high expression of most of the genes involved in proliferation and DNA repair with the exception of *NHEJ1* and *DNTT*, which had very low expression in all cell lines. The stem cell markers had very heterogeneous expression in all lines. Many downstream genes of the p53 signaling pathway had high expression in almost all cell lines. *CCND2* showed heterogeneous expression in different lines and *GADD45G* had very low expression in all lines. It seemed that genes involved in $Ca^{2+}$ rises or ER stress induced apoptosis, such as *BAD* and *BAX*, were homogeneously highly expressed in all lines, whereas the other apoptotic related genes were quite differently expressed. Adhesion molecules and molecules involved in the mobility were very inhomogeneous in their expression. Notably, the line 12370 had a specific lower expression pattern, being in line with its partly adherent and partly suspended growth pattern. Other cancer related genes showed different expression patterns in each cell line. *HER2 (ERBB2)* and *CA125 (MUC16)* had high expression in all lines. *ESR1* was not detected in the matched cell lines and *MPO* expression was generally low. Notably, the two lines derived from the same patient exhibited the smallest distance, constituting a cluster apart from all other cell lines. Interestingly, lines 13914_1 and 14433_1, bearing *BRCA1* and *BRCA2* mutation respectively, formed a separated cluster as well.

*Antigen expression of the cell lines and the corresponding tumors*

Antigen expression of the established cell lines was compared with the staining in the corresponding tumor tissues (Table 3).

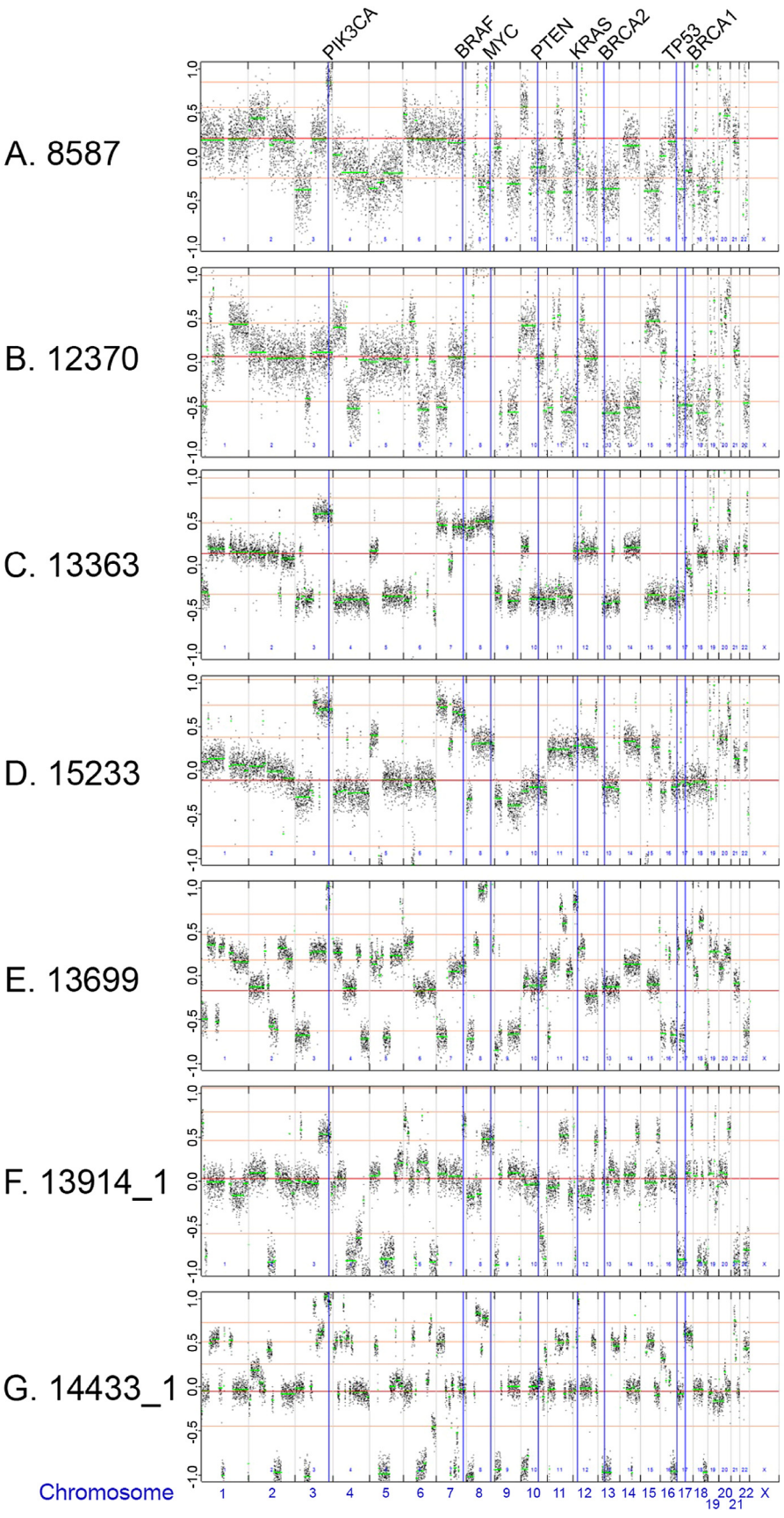


**Fig. 4.** Results of the low coverage whole genome sequencing of the cell lines. Blue lines indicate the positions of the specific genes indicated at the top of the graphic. Red lines represent an estimation of the neutral copy number level in each cell line. The light salmon lines represent the estimations of the alternative copy number levels (i.e. the first, the second and the third lines above the red line indicate amplifications with copy numbers 3, 4, 5, respectively, and the line below indicates a deletion with copy number 1).

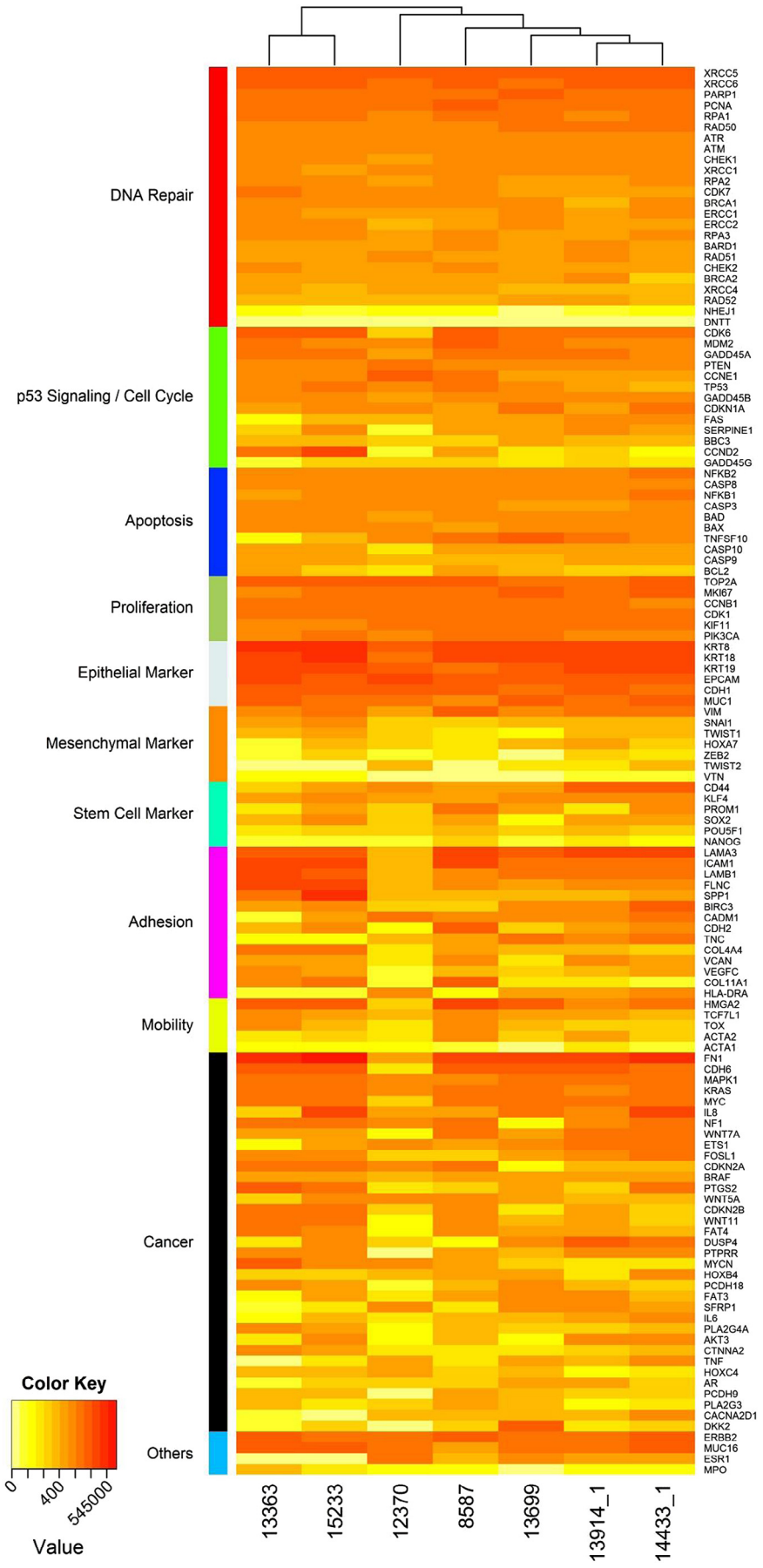


**Fig. 5.** Transcriptomic landscape of the cell lines. Values in the color key refer the read counts of gene expression.

**Table 3**
Score of the immunohistochemistry staining.

| Antibody | 12370 | | 13363 | | 15233 | 13699 | | 13914_1 | | 14433_1 | | 8587 | |
|---|---|---|---|---|---|---|---|---|---|---|---|---|---|
| | Cell line | TT | Cell line | TT | Cell line | Cell line | TT | Cell line | TT | Cell line | TT | Cell line | TT |
| Cytokeratin 8,18,19 | 4 | 2 | 4 | 4 | 4 | 4 | 4 | 4 | 4 | 4 | 2 | 4 | 4 |
| EpCAM | 4 | 2 | 4 | 4 | 4 | 4 | 4 | 4 | 2 | 4 | 2 | 4 | 4 |
| CA125 | 4 | 2 | 4 | 1 | 3 | 4 | 4 | 4 | 4 | 4 | 4 | 4 | 0 |
| Vimentin | 3 | 0 | 1 | 3 | 3 | 3 | 0 | 4 | 2 | 4 | 0 | 4 | 2 |
| CD44 | 4 | 1 | 1 | 1 | 0 | 3 | 3 | 4 | 1 | 4 | 3 | 0 | 1 |

TT = tumor tissue; 0: no expression; 1: weak expression in the minority of the cells; 2: weak expression in the majority of the cells; 3: strong expression in the minority of the cells, 4: strong expression in the majority of the cells.

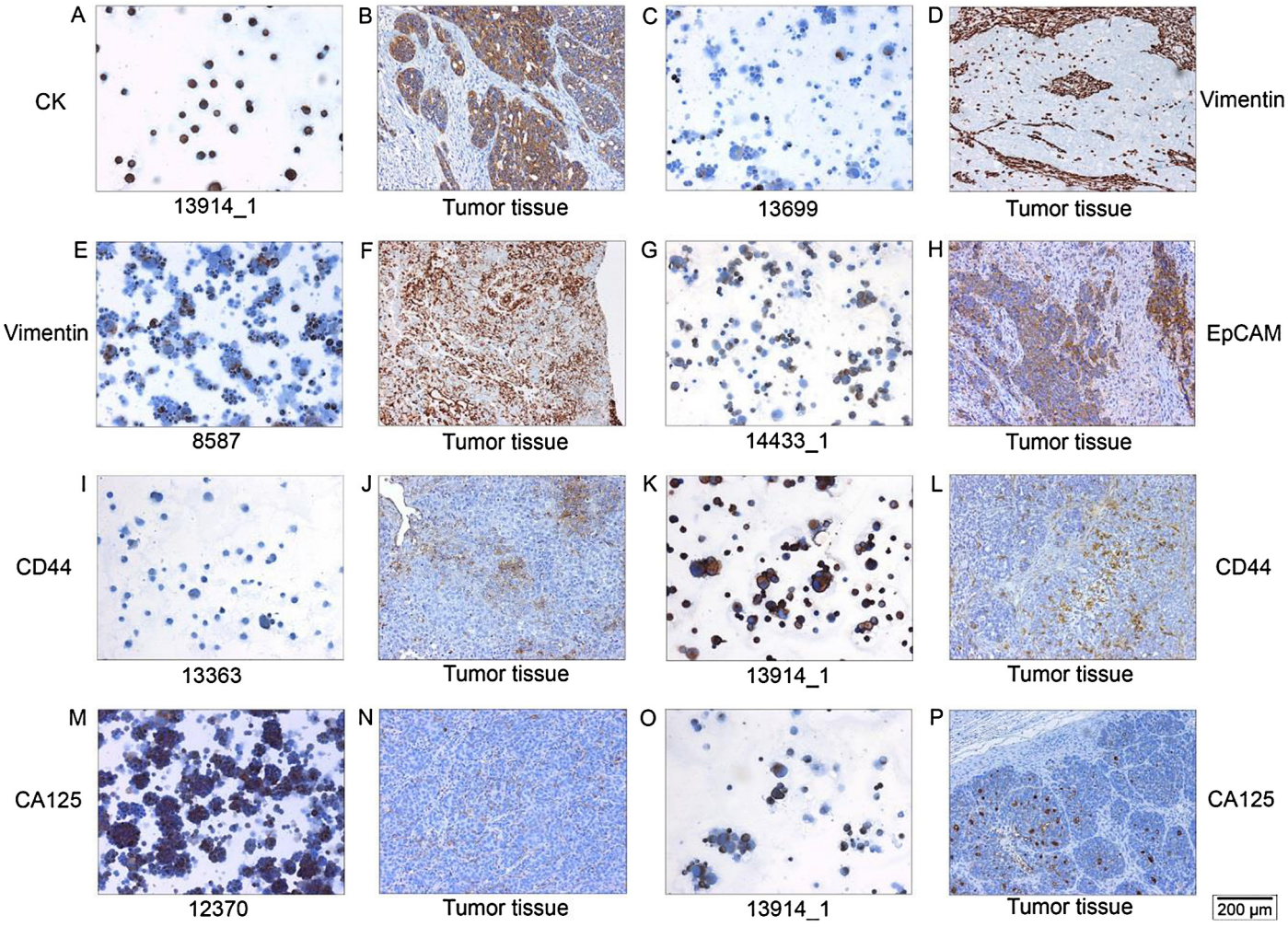


**Fig. 6.** Examples of immunohistochemistry staining from cell lines and the corresponding tumor tissues (brightfield microscopy).

Cytokeratins 8/18/19 and EpCAM were expressed in all tumor cells in tissues as well as in the cell lines (Fig. 6A,B,G,H).

CA125 was expressed in the majority of the cell lines as well as in tumor tissues (Fig. 6M–P).

Most of the patients had very few CD44 and Vimentin positive tumor cells in tissues (Fig. 6D,F,J,L). In the cell lines, the expression of these two proteins was quite heterogeneous (Fig. 6C,E,I,K).

In vitro *chemosensitivity*

Five cell lines did not show any remarkable differences in the responsiveness to carboplatin, all being highly sensitive to the drug. Two cell lines 13914_1 and 15233 were highly resistant (Fig. 7).

## Discussion

Experimental models are very important to study the cellular and molecular mechanisms underlying HGSOC. At the Helene Harris Memorial Trust meeting on ovarian cancer held in 2011, findings in basic, translational and clinical research were summarized and discussed by leading researchers in this field. Within the recommendations proposed for further research, better experimental models were requested as one of the most important issues [34]. As different histological types of ovarian cancers have been confirmed as being derived and driven from different molecular mechanisms, it is essential to have cell line models with defined pathological indications. In this work, we successfully established

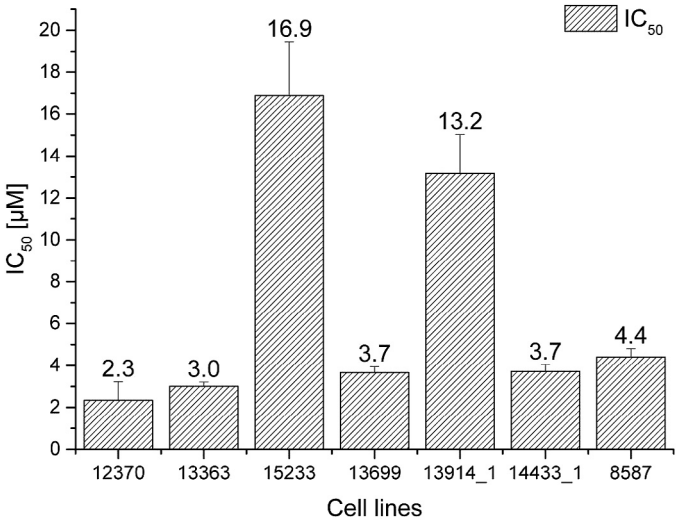


**Fig. 7.** IC 50 ± SD [µM] values of cell lines in response to carboplatin.

seven cell lines from HGSOC and provided the major genomic alterations and the transcriptomic landscapes of them. Every cell line was confirmed to consist of pure tumor cells, all harboring a unique *TP53* mutation corresponding to that of the original tumor and expressing cytokeratins 8/18/19 and EpCAM. Two cell lines were derived from the same patient, one was established before treatment and is sensitive to carboplatin, while the other was established during the second line chemotherapy and is highly resistant. Two cell lines were derived from germline *BRCA* mutation carriers, one of which also had breast cancer. This panel of cell lines is not only genetically and pathologically well defined, but they also have the uniqueness that all donors were treated with standard therapy.

Ovarian cancer is being recognized as a disease with distinct molecular backgrounds [35]. Seventy-five percent of EOC are of the high-grade serous type, making it a very important research target. However, most of our knowledge on ovarian cancer was generated from cell line models, which were neither well defined nor molecularly well characterized. An overwhelming number of publications on ovarian cancer were based on cell lines, which were "most unlikely high grade serous" [16]. Several current works [18,36] have been compiled which were based on three sets of matched cell lines established in the late 1980s [19]. Matched cell lines established from primary and recurrent tumor materials obviously provide new opportunities to study chemoresistance. Of the three cell line series, the first originated from low grade serous ovarian cancer, the second from a high grade carcinoma but without histopathological indication, and in the third series, all the cell lines were generated from ascites undergoing chemotherapy. It was argued that the detection of the *TP53* mutation could be an indicator of the high grade serous histological type [18], which is supported by other cellular and molecular analyses [37]. Molecular characteristics may help us to interpret the data generated previously. However, pathology is still a very important component to study the mechanisms of the disease. In reality, *TP53* mutations do not only occur in HGSOC, they are also detected in clear cell and mucinous tumors [38]. Confirmed by experienced pathologists, all cell lines established in our study were from HGSOC, thus providing a solid basis for further research.

Currently, the combination of carboplatin and paclitaxel is the standard first line therapy for primary HGSOC [34]. All cell lines in our study were established from patients receiving standard treatment, providing another advantage, which other recently established or used cell lines do not have [19–21].

Furthermore, two of our cell lines presented respective *BRCA1* and *BRCA2* mutations, each leading to a truncated protein. The *BRCA1* deficient cell line 13914_1 presented a highly resistant phenotype against carboplatin, while the *BRCA2* mutant cell line 14433_1 was sensitive. Cancer cells with *BRCA* mutations were known to be hypersensitive to DNA cross-linking drugs [39]. Hence, our two *BRCA* mutated cell lines certainly provide very valuable models to further study the role of *BRCA* genes and DNA repair mechanisms in chemoresistance.

In summary, we established seven cell lines from HGSOC. They all harbor specific *TP53* mutation as their corresponding tumors and express cytokeratins 8/18/19 and EpCAM. Two lines are from the same patient, one being established at diagnosis and sensitive to carboplatin and the other during chemotherapy and resistant to carboplatin. Two cell lines have *BRCA* mutations. Taken together, these cell lines are optimal models to investigate the molecular mechanisms underlying the progression, treatment resistance and recurrence of HGSOC.

## Acknowledgements

This project was partly supported by the grant from the European Union Seventh Framework Programme OCTIPS (Ovarian Cancer Therapy – Innovative Models Prolong Survival; Project Nr.: 279113) and the fellowship FEMtech from the Austrian Research Promotion Agency (FFG) Project "MCOvarianCancer" (Molecular characterization of ovarian cancer cells in ascites and tumor tissues; Project Nr.: 839939). Parts of this work were documented in the master thesis of Caroline Kreuzinger at the University of Vienna: "*Establishment and molecular characterisation of high grade serous epithelial ovarian cancer cell lines*" (2014). We thank Mrs Eva Schuster, Mrs Daniela Muhr, Mrs Christine Rappaport, Mrs Barbara Holzer, Ms Barbara Rath, Mrs Grazyna Dudek, Mrs Josefine Stani from the Medical University of Vienna (Vienna, Austria) and Dr. Michael Novy from the ViennaLab Diagnostics GmbH (Vienna, Austria) for their excellent technical support. We also thank Dr. Charles Theillet for his critical reading of the manuscript.

## Conflict of interest

None.

## References

[1] A. Jemal, R. Siegel, J. Xu, E. Ward, Cancer statistics, 2010, CA Cancer J. Clin. 60 (2010) 277–300.
[2] M. Kobel, S.E. Kalloger, D.G. Huntsman, J.L. Santos, K.D. Swenerton, J.D. Seidman, et al., Differences in tumor type in low-stage versus high-stage ovarian carcinomas, Int. J. Gynecol. Pathol. 29 (2010) 203–211.
[3] A. Rainczuk, J.R. Rao, J.L. Gathercole, N.J. Fairweather, S. Chu, R. Masadah, et al., Evidence for the antagonistic form of CXC-motif chemokine CXCL10 in serous epithelial ovarian tumours, Int. J. Cancer 134 (2014) 530–541.
[4] R.C. Bast Jr., B. Hennessy, G.B. Mills, The biology of ovarian cancer: new opportunities for translation, Nat. Rev. Cancer 9 (2009) 415–428.
[5] L. Galluzzi, L. Senovilla, I. Vitale, J. Michels, I. Martins, O. Kepp, et al., Molecular mechanisms of cisplatin resistance, Oncogene 31 (2012) 1869–1883.
[6] S.F. Bellon, J.H. Coleman, S.J. Lippard, DNA unwinding produced by site-specific intrastrand cross-links of the antitumor drug cis-diamminedichloroplatinum(II), Biochemistry 30 (1991) 8026–8035.
[7] T.A. Kunkel, D.A. Erie, DNA mismatch repair, Annu. Rev. Biochem. 74 (2005) 681–710.
[8] K.A. Olaussen, A. Dunant, P. Fouret, E. Brambilla, F. Andre, V. Haddad, et al., DNA repair by ERCC1 in non-small-cell lung cancer and cisplatin-based adjuvant chemotherapy, N. Engl. J. Med. 355 (2006) 983–991.
[9] S. Aebi, B. Kurdi-Haidar, R. Gordon, B. Cenni, H. Zheng, D. Fink, et al., Loss of DNA mismatch repair in acquired resistance to cisplatin, Cancer Res. 56 (1996) 3087–3090.
[10] W. Sakai, E.M. Swisher, B.Y. Karlan, M.K. Agarwal, J. Higgins, C. Friedman, et al., Secondary mutations as a mechanism of cisplatin resistance in BRCA2-mutated cancers, Nature 451 (2008) 1116–1120.
[11] I. Vitale, L. Galluzzi, M. Castedo, G. Kroemer, Mitotic catastrophe: a mechanism for avoiding genomic instability, Nat. Rev. Mol. Cell Biol. 12 (2011) 385–392.

[12] L. Galluzzi, E. Morselli, O. Kepp, I. Vitale, M. Pinti, G. Kroemer, Mitochondrial liaisons of p53, Antioxid. Redox Signal. 15 (2011) 1691–1714.
[13] Cancer Genome Atlas Research Network, Integrated genomic analyses of ovarian carcinoma, Nature 474 (2011) 609–615.
[14] M.J. Kwon, Y.K. Shin, Regulation of ovarian cancer stem cells or tumor-initiating cells, Int. J. Mol. Sci. 14 (2013) 6624–6648.
[15] F. Jacob, S. Nixdorf, N.F. Hacker, V.A. Heinzelmann-Schwarz, Reliable in vitro studies require appropriate ovarian cancer cell lines, J. Ovarian Res. 7 (2014) 60.
[16] S. Domcke, R. Sinha, D.A. Levine, C. Sander, N. Schultz, Evaluating cell lines as tumour models by comparison of genomic profiles, Nat. Commun. 4 (2013) 2126.
[17] M.S. Anglesio, K.C. Wiegand, N. Melnyk, C. Chow, C. Salamanca, L.M. Prentice, et al., Type-specific cell line models for type-specific ovarian cancer research, PLoS ONE 8 (2013) e72162.
[18] S.L. Cooke, C.K. Ng, N. Melnyk, M.J. Garcia, T. Hardcastle, J. Temple, et al., Genomic analysis of genetic heterogeneity and evolution in high-grade serous ovarian carcinoma, Oncogene 29 (2010) 4905–4913.
[19] S.P. Langdon, S.S. Lawrie, F.G. Hay, M.M. Hawkes, A. McDonald, I.P. Hayward, et al., Characterization and properties of nine human ovarian adenocarcinoma cell lines, Cancer Res. 48 (1988) 6166–6172.
[20] I.J. Letourneau, M.C. Quinn, L.L. Wang, L. Portelance, K.Y. Caceres, L. Cyr, et al., Derivation and characterization of matched cell lines from primary and recurrent serous ovarian cancer, BMC Cancer 12 (2012) 379.
[21] V. Ouellet, M. Zietarska, L. Portelance, J. Lafontaine, J. Madore, M.L. Puiffe, et al., Characterization of three new serous epithelial ovarian cancer cell lines, BMC Cancer 8 (2008) 152.
[22] G.J. Rustin, I. Vergote, E. Eisenhauer, E. Pujade-Lauraine, M. Quinn, T. Thigpen, et al., Definitions for response and progression in ovarian cancer clinical trials incorporating RECIST 1.1 and CA 125 agreed by the Gynecological Cancer Intergroup (GCIG), Int. J. Gynecol. Cancer 21 (2011) 419–423.
[23] H. Deissler, A. Kafka, E. Schuster, G. Sauer, R. Kreienberg, R. Zeillinger, Spectrum of p53 mutations in biopsies from breast cancer patients selected for preoperative chemotherapy analysed by the functional yeast assay to predict therapeutic response, Oncol. Rep. 11 (2004) 1281–1286.
[24] J.M. Flaman, T. Frebourg, V. Moreau, F. Charbonnier, C. Martin, P. Chappuis, et al., A simple p53 functional assay for screening cell lines, blood, and tumors, Proc. Natl. Acad. Sci. U.S.A. 92 (1995) 3963–3967.
[25] M.K. Tea, R. Kroiss, D. Muhr, C. Fuerhauser-Rappaport, P. Oefner, T.M. Wagner, et al., Central European BRCA2 mutation carriers: birth cohort status correlates with onset of breast cancer, Maturitas 77 (2014) 68–72.
[26] M. Wachtel, T. Runge, I. Leuschner, S. Stegmaier, E. Koscielniak, J. Treuner, et al., Subtype and prognostic classification of rhabdomyosarcoma by immunohistochemistry, J. Clin. Oncol. 24 (2006) 816–822.
[27] I. Scheinin, D. Sie, H. Bengtsson, M.A. van de Wiel, A.B. Olshen, H.F. van Thuijl, et al., DNA copy number analysis of fresh and formalin-fixed specimens by shallow whole-genome sequencing with identification and exclusion of problematic regions in the genome assembly, Genome Res. 24 (2014) 2022–2032.
[28] P. Van Loo, S.H. Nordgard, O.C. Lingjaerde, H.G. Russnes, I.H. Rye, W. Sun, et al., Allele-specific copy number analysis of tumors, Proc. Natl. Acad. Sci. U.S.A. 107 (2010) 16910–16915.
[29] D. Kim, G. Pertea, C. Trapnell, H. Pimentel, R. Kelley, S.L. Salzberg, TopHat2: accurate alignment of transcriptomes in the presence of insertions, deletions and gene fusions, Genome Biol. 14 (2013) R36.
[30] B. Langmead, S.L. Salzberg, Fast gapped-read alignment with Bowtie 2, Nat. Methods 9 (2012) 357–359.
[31] D. Risso, K. Schwartz, G. Sherlock, S. Dudoit, GC-content normalization for RNA-Seq data, BMC Bioinformatics 12 (2011) 480.
[32] S. Anders, W. Huber, Differential expression analysis for sequence count data, Genome Biol. 11 (2010) R106.
[33] C. Korch, M.A. Spillman, T.A. Jackson, B.M. Jacobsen, S.K. Murphy, B.A. Lessey, et al., DNA profiling analysis of endometrial and ovarian cell lines reveals misidentification, redundancy and contamination, Gynecol. Oncol. 127 (2012) 241–248.
[34] S. Vaughan, J.I. Coward, R.C. Bast Jr., A. Berchuck, J.S. Berek, J.D. Brenton, et al., Rethinking ovarian cancer: recommendations for improving outcomes, Nat. Rev. Cancer 11 (2011) 719–725.
[35] M. Shih Ie, R.J. Kurman, Ovarian tumorigenesis: a proposed model based on morphological and molecular genetic analysis, Am. J. Pathol. 164 (2004) 1511–1518.
[36] C.K. Ng, S.L. Cooke, K. Howe, S. Newman, J. Xian, J. Temple, et al., The role of tandem duplicator phenotype in tumour evolution in high-grade serous ovarian cancer, J. Pathol. 226 (2012) 703–712.
[37] C.M. Beaufort, J.C. Helmijr, A.M. Piskorz, M. Hoogstraat, K. Ruigrok-Ritstier, N. Besselink, et al., Ovarian Cancer Cell Line Panel (OCCP): clinical importance of in vitro morphological subtypes, PLoS ONE 9 (2014) e103988.
[38] M. Rechsteiner, A.K. Zimmermann, P.J. Wild, R. Caduff, A. von Teichman, D. Fink, et al., TP53 mutations are common in all subtypes of epithelial ovarian cancer and occur concomitantly with KRAS mutations in the mucinous type, Exp. Mol. Pathol. 95 (2013) 235–241.
[39] W.D. Foulkes, BRCA1 and BRCA2: chemosensitivity, treatment outcomes and prognosis, Fam. Cancer 5 (2006) 135–142.